Composite films containing red onion skin extract as intelligent pH indicators for food packaging

Elisa Boccalon [a], Gianluca Viscusi [a], Elena Lamberti [a], Fabio Fancello [b], Severino Zara [b], Paola Sassi [c], Maura Marinozzi [d], Morena Nocchetti [d], Giuliana Gorrasi [a*]*

[a] Department of Industrial Engineering, University of Salerno, Via Giovanni Paolo II, 132, 84084 Fisciano, SA, Italy
[b] Department of Agricultural Sciences, University of Sassari, 07100, Sassari, SS, Italy
[c] Department of Chemistry, Biology and Biotechnology, University of Perugia, Via Elce di Sotto, 8, 06123 Perugia, Italy
[d] Department of Pharmaceutical Sciences, University of Perugia, Via del Liceo 1, 06123 Perugia, Italy
* email: morena.nocchetti@unipg.it; ggorrasi@unisa.it

Abstract

A multifunctional and sustainable packaging was developed based on a potato starch matrix loaded with a cyanidin-rich freeze-dried onion extract (OE) anchored on a halloysite-layered double hydroxide filler. Due to a distinct colour change that varies according to the environmental pH, the extract acts as a visual sensor of food quality and is stabilised by the filler which, can be loaded with antibacterial agents, providing the active component of the film. In this work, the physical, mechanical and antimicrobial properties of films prepared with only extract or containing both extract and filler are examined and compared. In addition, the real-time sensing capability of the films was tested by monitoring their colour changes when applied in meat and milk storage.

Keywords: Sustainable packaging, Onion extract, Halloysite, Layered double hydroxides, pH indicator

1. Introduction

For years, the main requisites of ideal food packaging have been summarised by the formula: *protection*, *communication*, *convenience* and *containment* [1]. Traditionally, *communication* means the presence of labels indicating the content, traceability or nutritional values of food. Nowadays, communication is not a mere description of contents anymore, but has taken on an active value. Active communication implies the transfer of information from the product to the consumer to have constant control over the conditions of the food and its deterioration. These are the premises for implementing *intelligent* packaging. Intelligent packaging solutions span from biosensors (i.e., antibodies) to optochemical sensing methods (e.g., pH dyes, time-temperatures indicators), microwave doneness indicators (MDI), radiofrequency identification devices (RFID), etc. [2]. Whereas RFID and MDIs are designed specifically for traceability and distribution purposes, real-time information on food freshness is commonly assigned to optochemical systems. Among them, pH-sensing indicators, responsive to the total volatile basic nitrogen content or ammonia, and thiobarbituric acid reactive substances [3] have been successfully tested in monitoring the quality of seafood [4–6], meat, milk [7], and vegetables [8]. One of the hurdles of intelligent packaging consists in balancing the reliability of the detection system with the costs of such a solution. Another essential requirement is to ensure the absence of toxicity of the substances used as sensors and to avoid the contamination of the product with these compounds. For these reasons, natural dyes, like curcumin and anthocyanins, have attracted interest as viable substitutes for synthetic indicators like bromothymol blue, methyl red, [8] or polydiacetylene polymers [7].

Most films with pH-sensing properties lack in antibacterial functions, as they are essentially intended to convey information to customers and stakeholders for decision-making purposes. However, innovative solutions include packaging with even more advanced functionalities, designated as smart. *Smart* packaging combines interactive product-consumer communication with an active technology that offers a preservative action. Therefore, smart packaging is considered a ‘total packaging solution’[9].

Finally, further evolution of packaging is to combine smart functionality with sustainable solutions that could be a viable replacement for petroleum-based plastics. Thus, research has focused on introducing biodegradable polymers and recycling food waste.

With the aim of meeting the needs of a sustainable and total packaging concept, we designed potato starch films containing a filler based on halloysite nanotubes (HNT) decorated with layered double hydroxides platelets (LDH) [10] having both the function of carrier for active molecules and support for a natural dye to be used as a pH indicator. The pH sensor immobilized on the filler consists of a cyanidin-rich extract obtained from red onion dry skins. The interactions established between the extract and the filler surface are relevant to stabilize the colour of the film upon exposure to different pHs. In this work, films containing the filler-extract mixture were characterized (i.e. by evaluating thermal, optical, mechanical behaviour, and antioxidant and antibacterial properties) and tested as sensors for freshness detection of different food items. Results were compared to those obtained from films prepared with the extract alone. The real-time sensing capability of this compound was found to be efficient in revealing the change in products that generate both acidic and basic environments during spoilage.

2. Materials and Methods

Synthesis of HNT@LDH: The synthesis and deposition of LDH crystals on HNT to obtain the HNT@LDH composite was carried out with a solvent-free technique [10,11] wherein the salts of the metals of LDH were milled with the HNT nanotubes and NaOH in pellets by means of a ball mill.

The empirical formula of LDH, determined with ICP-OES measurements, is: $[Mg_{0.60}Al_{0.40}(OH)_2](NO_3)_{0.40}\cdot 0.2H_2O$.

Intercalation of salicylate in HNT@LDH: 750 mg of HNT@LDH were dispersed in a 0.1 M solution of sodium salicylate. The volume of salicylate was calculated so that the $mmol_{NO3^-}$/ $mmol_{Sal}$ ratio was stoichiometric. The sample was stirred for 1h, then washed once with deionised water and twice with acetone and dried at 60°C.

Preparation of starch film containing onion extract (OE): a 5% (w/v) potato starch solution was heated up to 90°C to dissolve the starch. Glycerol (20% w/w) was used as a plasticizer. The mixture was cooled down and added to a 0.1% (w/v) dispersion of OE in distilled water. The composite was transferred to a Teflon plate and dried at 40°C for 24 h. A red film was obtained referred to as MOE. A reference film, constituted by plain starch and glycerol, was prepared as described above and named M0.

Preparation of starch film containing OE and HNT@LDH: the same procedure described for preparing MOE was used for the obtainment of composite films containing the filler and OE (FOE) and the filler loaded with salicylate and OE (SOE). OE was anchored to the filler alone or to the filler loaded with salicylate by grinding HNT@LDH and OE in a 10:1 (w/w) ratio using a mortar and a pestle. The 1% (w/v) dispersions containing FOE and SOE, respectively, were added to the potato starch solution and mixed until fully homogenized. Both composite films, named MFOE and MSOE, respectively, were green.

pH detection ability of films: the colour of the extract is expected to change from red to green going from neutral to basic conditions. MOE is originally red and was used without further manipulation. MFOE and MSOE are instead green (MFOE/G and MSOE/G, respectively) and were maintained in a desiccator in the presence of acidic fumes for 15 minutes to turn them into red films (MFOE/R and MSOE/R).

On the other hand, the films are expected to shift from green to pink by moving from neutral to acidic conditions. Thus, to detect pH changes from neutral to acidic conditions, MOE was maintained in a desiccator in the presence of ammonia fumes to obtain a green film as a starting material (MOE/G) while MFOE and MSOE were used as-prepared.

X-ray powder diffraction: X-ray powder diffraction (XRPD) patterns were collected with the Cu-Kα radiation on a Bruker D8 Advance diffractometer and PW3050 goniometer, equipped with a Lynxeye detector. The long fine focus (LFF) ceramic tube was operated at 40 kV and 40 mA.

ATR Measurements: Infrared spectra of the samples were collected using a Fourier transform (FT-IR) Alpha instrument from Bruker Optics and its ATR (Attenuated Total Reflection) module equipped with a diamond crystal. The spectra were collected in triplicate in the 4000-400 cm^{-1} spectral range with 30 scans and an average resolution of 2 cm^{-1}. The samples were analyzed as prepared.

Raman Measurements: Raman measurements were carried out by means of a MonoVista CRS+ Raman spectrometer connected to an Olympus Inverted IX73 microscope equipped with a 50X long focal length objective. The materials were analyzed using red laser radiation at 785 nm as excitatory sources. The spectra were recorded with the maximum laser power allowed by the instrument, i.e. 13.600 mW, 20s of acquisition and 30 accumulations, using the 300 line/mm diffraction grating and setting the slit aperture at 70 μm. The measurements were repeated three times for each sample.

Thermogravimetric analysis: Thermogravimetric analysis (TGA) were performed with a Mettler TC-10 thermobalance. Measurements were collected from 25 to 700°C, at a heating rate of 10°C/min in an air atmosphere.

Transparency measurements: Light barrier properties were assessed by an UV–vis measurements using a UV-2401 PC Shimadzu (Japan) spectrophotometer. Film samples of 0.8 cm × 4 cm were cut and the light transmission was measured in the 200– 800 nm ranges. The transmission value was recorded at λ=600 nm and measures were repeated in triplicate. The transparency of the films was calculated using the following equation:

$$Transparency\ value\ (Tr) = {}^{-log(T_{600})}/_{x}$$

Where T_{600} corresponds to the Transmittance value at 600 nm, and x is the film thickness (mm). The higher the transparency index value, the lower is the transparency of the film [12].

Water contact angle: Contact angle measurements (WCA) were carried out using a high-resolution camera. Droplets of distilled water were dispensed on a 1 × 1 cm^2 test sample at room temperature. The contact angle was determined using Drop Analysis software. Five contact angle measurements were recorded at different points for each sample, and the average contact angle was determined.

Mechanical properties: Elastic moduli of the samples were obtained by means of a dynamometric apparatus INSTRON 4301. Experiments were conducted at room temperature at a deformation rate of 0.5 mm/min on 3 samples per film.

Antimicrobial activity of the OE and MFOE film: The bacterial pathogens tested in this work (*Escherichia coli* DSM 30083, *Listeria monocytogenes* DSM 20600 and *Salmonella bongori* DSM 13772) were obtained from the German Collection of Microorganisms and Cell Cultures GmbH DSMZ (Deutsche Sammlung von Mikroorganismen und Zellkulturen) and have been cultivated following manufacturing instructions. After revitalization, the freeze-dried pathogens cultures were stored at -80°C in Brain Heart Infusion (BHI) broth (Oxoid, Basingstoke, UK) plus 20% of glycerol.

When needed, the pathogens cultures were thawed and subcultured twice in BHI broth at 37 °C for 18 h to reach the early stationary phase (~9 log CFU/mL).

Stock solutions of OE (with a concentration of 25 mg/mL) were prepared in distilled sterile water.

The minimal inhibition concentration of OE was determined according to M07-A9 standard (Clinical and Laboratory Standards Institute, 2015). Stock solution was two-fold diluted in water into a series of final concentrations ranging from 12.5 and 0.012 mg/mL. Overnight pathogens cultures were then used to prepare microbial inocula for the test in 2x cation adjusted Muller Hinton broth (Oxoid, Basingstoke, England). Aliquots of 100 μL of diluted inocula at desired cells concentration were added to each well in the 96-well micro-dilution plate previously containing 100 μL of desired OE dilutions. Plates were then incubated at 37°C for 24 h. After incubation, MICs (mg/mL) values were determined as the lowest OE concentration that inhibited visible growth of the tested microorganism, which was indicated by absence of turbidity.

The antimicrobial activity of MFOE (6 mm of diameters) was also tested by the disc diffusion test. A disc of 30 μg of chloramphenicol (CPD, Thermo Scientific™, Oxoid™ Basingstoke, UK) and a paper disc (Whatman® Antibiotic Assay Discs, Darmstadt, Germany) were used as positive and negative control respectively. One hundred microliters of different pathogens cultures, obtained as above described, were spread on the surface of a petri dish contain 25 mL of BHI agar. The plates were left to dry for 1h and then two MFOE and a CPD disc were laid in the surface plates and then incubated for 24 h at 37°C. After incubation the diameter of inhibition was measured by means of a caliber.

DPPH radical scavenging assays: The antioxidant properties of the extract were investigated by performing radical scavenging assays in the presence of the free radical 2,2-diphenyl-1-picrylhydrazyl (DPPH). The efficiency of the scavenging action was determined by measuring the decrease in absorbance of DPPH solutions (λ=517 nm) containing different concentrations of antioxidant and compared to the initial absorbance from control assay. The parameter selected to quantify the radical scavenger activity is the concentration of substance required to reduce the DPPH absorbance by half (EC_{50}). The value of EC_{50} was calculated for both OE and FOE.

To obtain EC_{50} of powdered OE, a 100 ppm solution of OE was prepared by dissolving 5 mg of OE in 50 mL of water. Aliquots of the solution containing 0.007-0.05 mg/mL of OE were mixed with a 10^{-4} M solution of DPPH in methanol. The mixtures were kept in the dark at room temperature for 30 min and then the absorbance values were measured. Methanol was used as a blank. The EC_{50} determined for OE is 0.007 mg/mL.

EC_{50} estimation of powdered FOE was performed by weighting amounts of FOE containing 0.07-0.5 mg of OE (OE content in FOE= 9% w/w). The samples were mixed with a 10^{-4} M DPPH solution in methanol and maintained in the dark, under constant stirring, for 30 min. Before measuring the absorbance values, the solutions were filtered to remove the residues of the filler. EC_{50} of FOE is 0.009 mg/mL.

The antioxidant activity of MOE, MFOE and MSOE was monitored as a function of time. Disks of 0.6 cm diameter (28.3 mm^2) containing 0.02 mg of extract each were mixed with 100 µL of water and 2.9 mL of DPPH 10^{-4} M in methanol. The disks were maintained in the dark and constantly stirred. The decrease in absorbance was measured at given interval times and monitored for a total of four days.

3. Results and discussions

Before discussing the film characterizations, it seems useful, for reader convenience, to recall the main components of OE and their properties. According to HPLC measurements reported in a previous article [13], glycosylated quercetin (or isoquercetin, IQR) and cyanidin 3-O-(malonyl) glucoside (CMG), whose structures are reported in Figure 1(a), represents the major components of OE.

CMG gives to the extract a reddish colour that remains stable until a pH variation occurs. As the pH raises a shift from red (pH:3-7) to purple (pH:7-8) to green (pH>8) is evidenced in agreement with the conversion of the structure from flavylium cation to neutral and then to anionic quinonoid base, respectively. The main changes in structure derive form the progressive deprotonation of OH groups in either C5-7 or C3'-4' positions.

A colour shift from red to green is produced also by mincing OE with HNT@LDH. This colour variation can be attributed to the presence of carbonate ions on the surface of LDH which interact with cyanidin causing the deprotonation of the OH groups thus producing the quinonoid base form. Thus, FOE appears as a green powder. The presence of HNT@LDH has some influence on the stability of the form assumed by CMG.

MOE are originally red and turn green after being exposed to basic fumes; however, the as-obtained anionic quinonoid base form is not permanent: indeed, within 15 minutes cyanidin gets re-protonated by reaction with atmospheric CO_2 and the films resume a red hue. On the contrary, films prepared with FOE or SOE (MFOE and MSOE, respectively) are originally green and can be converted to red by exposition to acidic vapours. The protonated form is stable and the colour remains red unless the films come in contact with a basic environment.

The increased stability of CMG is related to the establishment of LDH-OE surface interactions: once the quinonoid base is formed, the catechol group of CMG is supposedly positioned facing the LDH surface as shown in Figure 1(c). This interaction is not affected by exposure to air, as in the case of

MOE, and can only be broken in the presence of acidic fumes. As a consequence, films containing FOE or SOE are more reliable as sensors than those prepared with OE alone.

A schematic illustration of the colour shift of MOE, MFOE and MSOE upon exposure to different environments is shown in Figure 1(d).

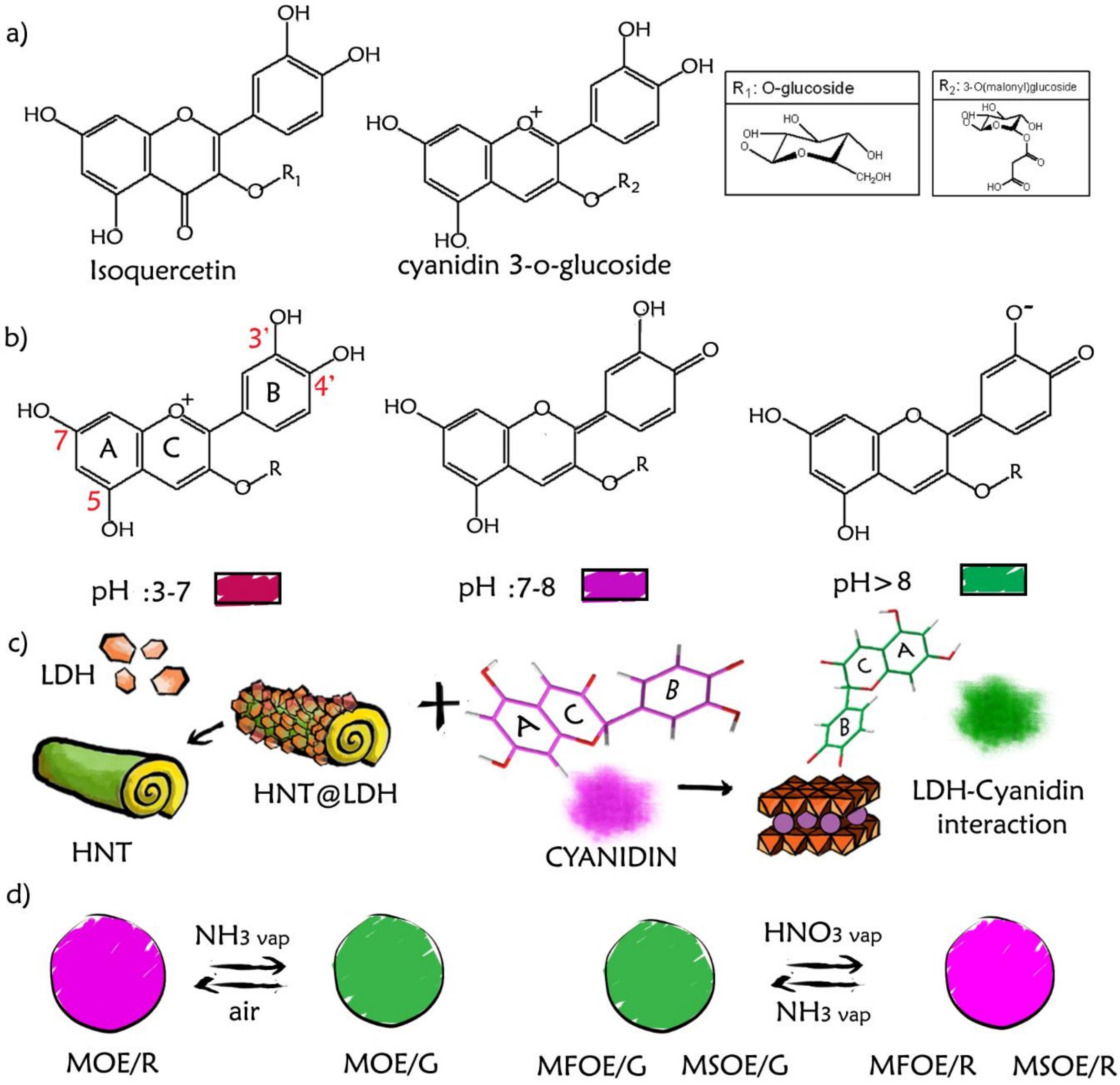

Figure 1. a) Structures of isoquercetin (IQR) and cyanidin 3-O(malonyl)glucoside (CMG); b) CMG forms at different pH values; c) representation of HNT@LDH filler and of the supposed LDH-cyanidin interaction; d) schematic representation of the colour change of MOE, MFOE and MSOE films as prepared and after exposure to acidic or basic fumes (R and G stand for red and green respectively and are used to distinguish the colour taken by the film upon exposure to acidic or basic environment).

Spectroscopic, physical, and mechanical characterizations of the films were performed by comparing the plain starch film, M0, with the properties of those prepared with extract only (MOE), extract-filler composite (MFOE), and salicylate-intercalated filler (MSOE), respectively.

The XRD patterns of the four films are shown in Figure 2(a). Diffraction peaks positioned at 2θ= 5.6°, 11°, 17°, 22° and 23° appear in all of them. These reflections are characteristic of the B-type crystallinity typically displayed by tubers [14]. Starch crystallinity is commonly reduced after the plasticization process, as glycerol interacts with the polymer molecules by disrupting the intermolecular hydrogen bonds. In this case though, the clear presence of the B-type pattern denotes that a semi-crystalline structure has been maintained. This is possible due to the realignment and re-association of the amylose and amylopectin chains occurring after fusion and gelatinization during the retro gradation process [14].

The incorporation of the filler is not accompanied by significant changes in the diffraction patterns. The absence of noticeable filler reflections suggests their homogeneous distribution within the polymer.

The films were further characterized using ATR and Raman spectroscopy. Figures 2 (b-d) show a comparison of the ATR and Raman spectra of the plain starch film with those of the MOE and MFOE composites (MSOE data are not shown because the spectra are coincident with those of MOE). As with the XRD patterns, the starch signals are dominant and no specific band can be attributed to the presence of the extract or filler. Specifically, the ATR profile of starch is distinguished by the presence of C-H and C-O deformations at 400-900 and 1200-1500 cm^{-1}, C-O-C antisymmetric stretching vibration at ca. 1160 cm^{-1}, C-H stretching modes at 2900 cm^{-1} and O-H vibrations at 3500 cm^{-1}. In the Raman spectra, the band at 485 cm^{-1} corresponds to the vibrational modes of the pyranose ring which is a marker for the amount of amylose and amylopectin in starch. The 800-1200 cm^{-1} region is characteristic of C-C, C-O and C-O-C deformation, and the strong band at ca. 940 cm^{-1} is typical of α-1,4 glycosidic linkage mode. COH and CH bending modes are observed in the region between 1370-1460 while and at 2900-2980 cm^{-1} CH stretching bands are evident [15,16]. IR absorption and Raman scattering have largely been used to follow the retrogradation process of starch, being their signals very sensitive to the structure of the polymer [16–18]. It has been reported that the structural differences of both starch materials can be detected in the C–H stretching region between 2700 and 3100 cm^{-1} [19]. Our data show that the four samples have very similar spectra and only a slight red-shift of CH stretching bands in the 2800-3000 cm^{-1} region was observed in MFOE, MSOE and MOE with respect to M0. This suggests that the presence of the filler and of OE does not drastically alter the structure of the film, but a weak increase of ordered structures probably takes place as already evidenced by XRD patterns.

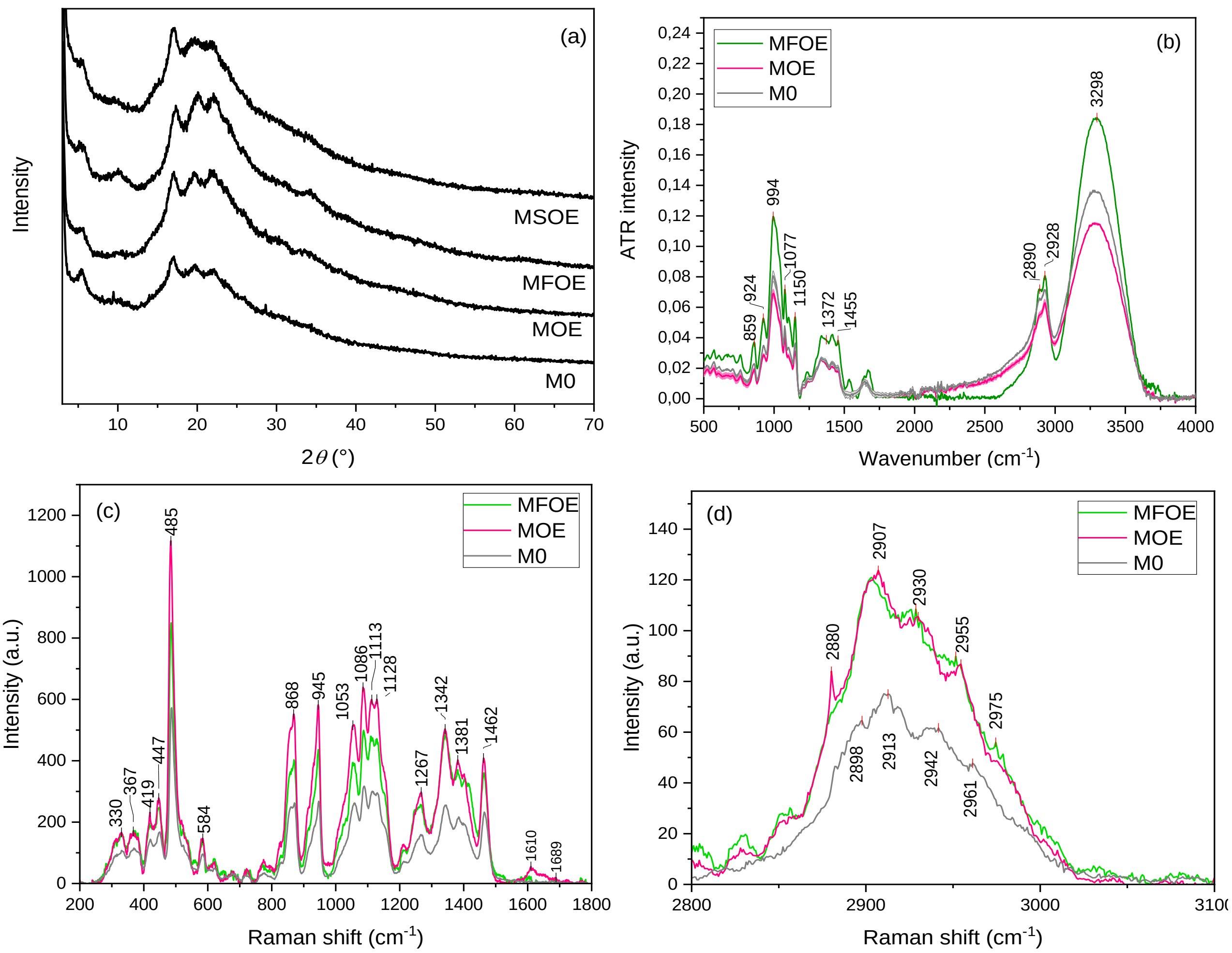

Figure 2. a) XRD patterns of the potato starch based films M0, MOE, MFOE and MSOE. b) ATR spectra of M0, MOE and MFOE. c-d) Raman spectra of M0, MOE and MFOE.

The degree of filler distribution within the polymer was best observed by collecting SEM images of MFOE. The cross-sectional image of the sample (Figure 3 (a)) reveals a granular surface due to the homogeneous presence of the filler in the polymer matrix, interrupted by some agglomerates, as shown in the magnification of Figure 3 (b). The homogeneity of the filler distribution is confirmed by the elemental mapping of Si and Mg carried out on the portion of the sample shown in Figure 3(c). These elements, which trace the presence of HNT and LDH (Figure 3(d)) respectively, are uniformly spread throughout the sample, also revealing that LDH is not separated from HNT.

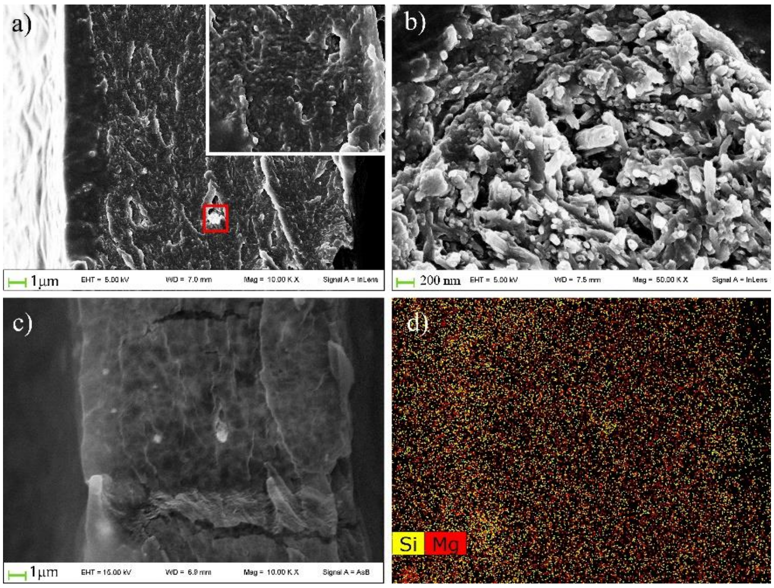

Figure 3. a) SEM image of MFOE, the inset reports a magnification of the sample; b) magnification of the agglomerate in the red square of (a) showing the HNT@LDH filler; c) Secondary electron image of the mapped area of the sample; d) elemental distribution of Si (HNT) and Mg (LDH).

Physical properties of the films

Physical characterization was performed by evaluating the thermal, optical and mechanical behaviour of the samples.

Thermogravimetric analysis: Weight loss and derivative thermogravimetric curves are illustrated in Figure 4. The TGA curve of M0 is divided into three steps: the first mass loss (below 100°C) is related to the evaporation of water; the second, from 150 to 300°C, corresponds to the starch degradation (i.e. inter/intramolecular dehydration and high-temperature pyrolysis) and to the elimination of the plasticizer; finally, above 300°C, the pyrolysis and degradation of the intermediate products occur [20].

The TGA profiles of MFOE and MSOE show the contribution of the decomposition of HNT, LDH and OE which mainly affect the degradation temperature of starch. This influence is better depicted in the DTG curves: the degradation temperature shifts from 282°C in M0 to about 300°C in MOE, while in MFOE and MSOE is set to 295 and 291°C, respectively, indicating that all the composites display enhanced thermal resistance. Factors influencing the thermal behaviour are the degree of clay dispersion, the number of exposed hydroxyl groups and the reorganization of the starch chains [21]. Inorganic fillers in general are known to improve the thermal properties of polymers by producing a barrier that slows down the heat transfer and this is the case with MFOE and MSOE. Conversely, the presence of OE, which is usually is associated to lower thermal stability, produces a shift to the highest value, reflecting a good cyanidin-starch interaction and a reduction of the exposed OH groups [22].

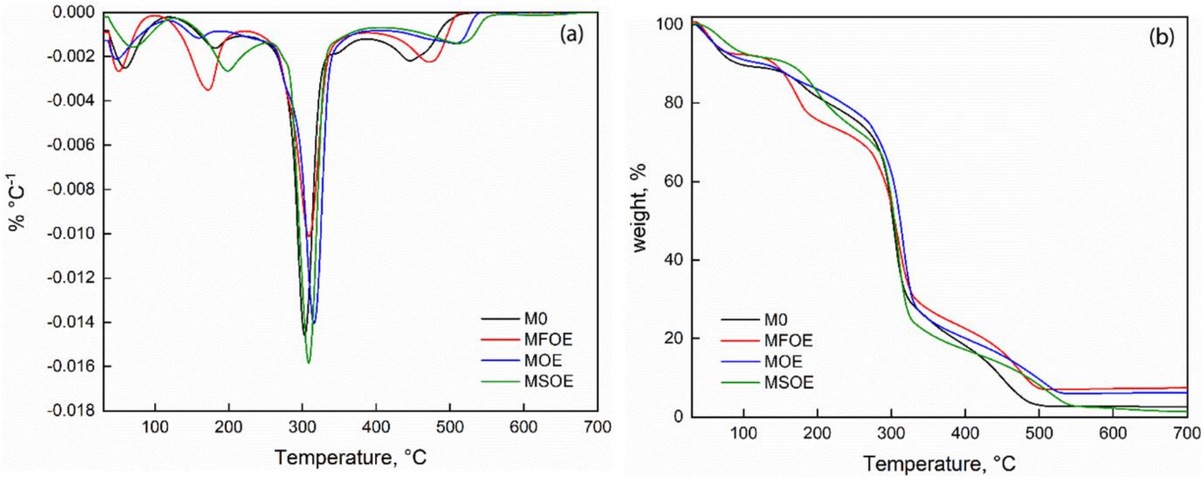

Figure 4. TGA (a) and DTG (b) curves of M0, MOE, MFOE and MSOE. Heating rate of 10°C/min in an air atmosphere.

Optical Transparency

Visually, the four films are very different in colour: M0 is white and opaque, MOE is pink, while MFOE and MSOE are characterized by two different shades of green. The order of optical transparency is: MFOE<MOE<M0<MSOE (Table 1). Compared to M0, MOE has a similar Tr index (Tr= 7 and 8, respectively), indicating that OE is evenly dispersed throughout the matrix. On the contrary, the presence of the filler changes the optical properties significantly; in MFOE the Tr value raises up to 14, and in MSOE is lowered to 3. An increment in opacity is generally expected when clay is added to polymers and this applies to MFOE. The extent of the Tr variation depends on the dimension, degree of dispersion and concentration of the nanoparticles, as well as on the compatibility of the filler with the polymer [23]. The values of transparency indices calculated for MSOE and MFOE for the same filler concentration and particle size are very different from each other. It is therefore possible to conclude that what mainly distinguishes the transparency value in the two samples is the presence of salicylate that generates a better dispersion of the crystals in the matrix resulting in a lower Tr index which is extremely important for a better product-consumer communication.

Water contact angle (WCA)

Water contact angle was measured for MOE, MFOE and MSOE and compared to control M0. This measure is important to evaluate the degree of hydrophilicity of the film. The pure starch film is the most hydrophilic one (WCA= 41°) due to the natural presence of numerous OH groups in the polymer chain (Table 1). Conversely, in MOE the contact angle increases, reaching 52°. This trend can be explained considering the composition of onion skin which contains a certain fraction of non-soluble fibres among which lignin [24] may be the main responsible component for the reduction in wettability. The hydrophobic nature of the films is even more pronounced in MFOE and MSOE, which display a contact angle of 60° and 62°, respectively, thereby evidencing that the presence of the filler enhances water repellency even more. The increment of hydrophobicity may be related to the building of interfacial interactions between the filler and the starch OH groups. These interactions partially hinder the rearrangements of the starch chains making them less susceptible to water contact. This behaviour is most evident for MSOE wherein the surface molecules of salicylate expose the phenyl moieties towards the polymer modifying the wettability towards a higher contact angle.

Mechanical properties

The parameters influencing the mechanical behaviour of the film are related to intrinsic characteristic of starch (e.g. molecular weight and amylose fraction) as well as to the specific properties of the film preparation (e.g. film thickness, filler content and crystallinity) [25]. Tensile tests performed on films revealed Young's modulus results in the 17- 41 MPa range (Table 1). The highest value (41 MPa) was obtained for M0, while the addition of the extract and the filler incredibly reduced the stiffness. From these results it can be deduced that, in MOE sample, OE interferes with the intramolecular linkages of polymer chains and leads to a decrease of the modulus [26]. The loss of cohesion can also be attributed to the presence of occasionally bigger particles in the powdered OE which create points of discontinuity within the film [27]. A little inhomogeneity in the composition of OE is to be expected as the product is not purified but derives directly from discarded onion skins.

An even lower value is reached in MFOE (17MPa); the filler seems to further weaken the intermolecular starch bonds. This behaviour may result from the stronger OE-filler interactions which induce the deprotonation of cyanidin and reduce the number of hydrogens in OE suitable for creating a network of H-bonds with the hydroxyl groups of starch [28]. An improvement is given by the presence of salicylate that is mainly involved in linkages with LDH surface, making the filler less amenable for the direct interaction with starch and favouring the polymer-polymer bondage.

Table 1. Optical transparency, water contact angle and elastic moduli values of the starch-based films.

Sample	Optical Transparency	Water Contact angle (°)	Elastic Modulus (MPa)
M0	7±0.6	41±2.1	41 ± 2.1
MOE	8±0.6	52±1.8	25 ± 2.2
MFOE	14±1.2	60±2.6	17 ± 1.2
MSOE	3±0.2	62±2.0	24 ± 1.8

Antibacterial activity of OE

Onion (Allium cepa L.) is one of the oldest and important crops from olden time. In addition to possessing many health benefits [29,30], several studies confirmed that onion skins contain high amount of quercetin and other quercetin derivatives which have been assessed as antifungal and antibacterial agents [31–34]. Hence, these natural compounds have attracted food industry as antimicrobial agents for improving food shelf life [35].

The OE analyzed in this work, showed good inhibitory activity against *Staphylococcus aureus* DSM 20231 with a MIC of 0.78 mg/mL in agreement with previous results obtained by Pagano et al. [13] and Sagar et al. [30] with bacteria belonging to the same species. OE also showed a strong inhibitory activity against *Listeria monocytogenes* DSM 20600 with a MIC of 0.39 mg/mL, that is lower than MIC value found for *Listeria innocua* also obtained by Pagano et al. [13] but higher than that obtained by Somrani et al. [36] It is known that the antimicrobial activity of natural compounds are species and strains dependent [37,38]. OE did not showed inhibitory activity against gram negative bacteria tested in this work, i.e. *Salmonella bongori* DSM 13772 and *Escherichia coli* DSM 30083. This result is partially in contrast with the results obtained by Sagar et al. [39], who found an antimicrobial activity of onion extracts against gram- bacteria, although the activity was dependent on the onion variety. Finally, MFOE showed an inhibitory activity only against *S. aureus* DSM 20231 (with a mean diameter of inhibition of 8.2 mm, including the diameter of the disc). No inhibition halos were observed against the other bacterial species tested. The differences in the antimicrobial activity of the extract compared to that of the MFOE could be due to the fact that of the filler itself retains the extract in the medium. It can be concluded that onion extracts, due to the presence of antimicrobial components can be considered good natural preservatives for the food sector as they could reduce the use of chemical products and be of interest to consumers.

Antioxidant activity of OE

Almost all molecules in the flavonoid class exhibit antioxidant activities. The mechanism of scavenging reaction involves the donation of a hydrogen atom to a radical. The donation is favoured by the presence of functionalities and conjugations that stabilize the flavonoid radical after the hydrogen loss [40].

The structural elements with the most favourable scavenging properties are a) the two vicinal hydroxy groups on $C_{3'}$ and $C_{4'}$ (catechol moiety) of ring B, b) C_3 and C_5 hydroxyl functionalities in ring C and

A, respectively, and c) the presence of the C_2-C_3 double bond conjugated with the C_4-oxo moiety [41].

Quercetin is endowed by this structural pattern. An ideal reaction of a fully protonated quercetin molecule with a radical can be described as follows: one hydrogen is first transferred from the catechol moiety to the radical and a stable flavonoid phenoxyl radical is formed. Then, the phenoxyl radical can react with another radical to give a quinone structure [42].

Glycosylation is known to reduce this activity. In our case, quercetin and cyanidin are both glycosylated, thus we expect a lower scavenging potential from OE. Other differences concern the activity of the pure extract compared to that of the extract mixed with the filler as in FOE.

In this case the number of hydrogens available for the antioxidant reaction may be reduced since cyanidin takes the form of an anhydrobase and supposedly interacts with the LDH surface either through the catechol moiety or the oxygen in $C_{5/7}$ position (Figure 1(c)). The first hypothesis should result in a lower antioxidant activity, as would be lacking the role played by the catechol hydrogens. This implies that the scavenging activity has to be compensated by the hydroxyl positioned in C_5 and C_7 of ring A [43].

To verify these hypotheses, the antioxidant activity of the OE and FOE was evaluated by DPPH assays. The EC_{50} values calculated for OE and FOE were 0.007 mg/mL and 0.009 mg/mL, respectively. The immobilization of OE on the filler causes, as expected, only a slight decrease of the antioxidant activity. Therefore, was of interest to verify the effect of the polymeric matrix on the antioxidant properties of OE in MOE, MFOE, MSOE.

Once the samples are incorporated in the polymer, diffusion factors influence the release of CGM and affect the antioxidant activity of the extract. As a consequence, the scavenging capability in the films was evaluated as a function of time and a comparison was made between the film containing only OE (MOE), the one with filler and OE (MFOE), and a film with filler, salicylate and OE (MSOE).

Figure 5 shows the percentage of residual DPPH plotted against the time. MOE exhibits the higher antiradical activity: 25% of the DPPH is scavenged in the first two hours and 40% in one day. After this rapid effect, the trend becomes slower and the activity decreases until the EC_{50} is reached in about three days. The faster reaction of MOE could be promoted by two factors: the first one is that the extract which is not combined with the filler is in a neutral anhydrobase form and has more hydrogens available for the scavenging of the DPPH radical; secondly, the extract does not get trapped in the polymeric network, instead, it migrates and is released from the film. For instance, when MOE is dipped in water, the water turns a pinkish hue. In MFOE, the interactions of the filler with CGM are stronger since OE, in addition to interacting with the surface of LDH, is also partially intercalated in it, and has less chance of reacting with the radical, thus the trend of DPPH bleaching proceeds slowly. EC_{50} is not reached even after three days. With a linear progression, it can be calculated that 50% of DPPH inhibition is only achieved in five days. MSOE falls in the middle: the interlayer space of LDH is occupied by salicylate anions and the extract is mainly on the surface and more easily released.

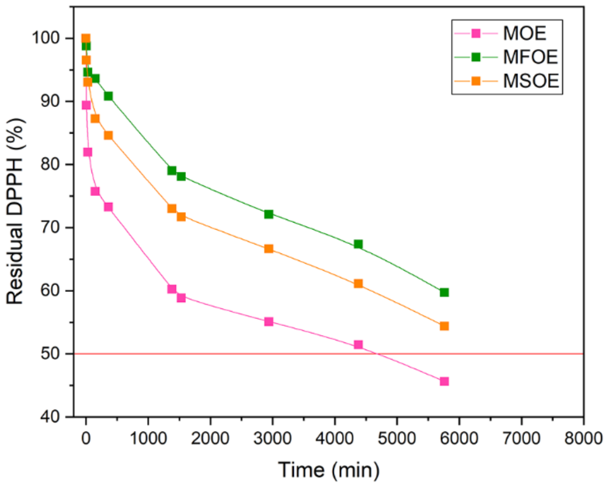

Figure 5. Kinetic behaviour of the radical scavenging action of MOE (pink squares), MFOE (green squares) and MSOE (orange squares).

Application of the films

The pH detection ability of cyanidin in MOE and MFOE was tested on perishable food items such as meat and milk. During decomposition, spoiled meat produces volatile amines that change the pH of the storage container to an alkaline environment. MOE was applied as prepared, instead MFOE was first placed in a desiccator saturated with HNO_3 fumes to protonate the cyanidin and obtain a red membrane (MFOE/R). Beakers filled with meat pieces were sealed with the films and stored in a refrigerator at 4°C. The colour of the membranes was checked repeatedly over the next 7 days. In the case of MOE, no change in colour was visible, even after 7 days (pictures not reported). This confirms what was previously observed with MOE/G: although the amines interact with cyanidin, ambient CO_2 and humidity reverse the reaction. As a consequence, the starch-based film containing only OE is not a proper indicator for food freshness.

On the other hand, in MFOE/R (Figure 6), the first changes are visible after three days: a green stain appears and spreads progressively along the entire package until, within 5 days, it becomes all green. As can be seen from the images in Figure 6, the speed of the reaction also depends on the thickness of the film: in thin films, the colour change spreads more quickly throughout the membrane.

Due to the stabilizing effect of the filler on the flavylium cation or the anhydrobase form of cyanidin, it is also possible to detect of acidic pH with the same MFOE film. To detect a change in pH from neutral to acidic, as prepared disks of MFOE, green coloured (MFOE/G), were applied to the inner caps of vials containing milk. Disks of MOE, previously exposed to ammonia vapor to obtain a green film (MOE/G), were also used for comparison. The vials were sealed and kept at room temperature. After 3 hours the caps were removed and the colour was checked. MOE/G had already turned pink, even though the pH of milk was still 6.8. In contrast, in MFOE/G, the colour conversion was only visible after 7 days, when the pH had reached 5.5. The same experiment was repeated with a vial half-filled with milk to simulate the real milk consumption conditions and verify whether the sensor ability to check the pH depended on the headspace of the container. No significant differences were noticed with respect to the vial completely filled with milk.

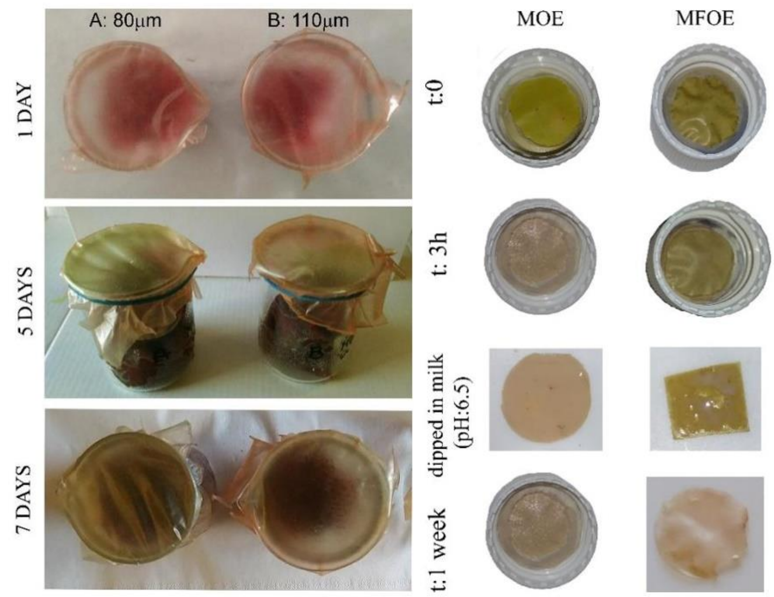

Figure 6. Images of the colour changes of MFOE film applied over beaker containing meat to monitor the freshness of meat over time (left). The difference between the two films is only in thickness: 80 and 110 μm respectively; cups with MOE and MFOE disks that sealed vials filled with milk (right).

4. Conclusions

Starch-based films prepared with the filler-OE compound meet the requirements for a smart packaging with the added value of sustainability. As well as reducing the potential harmful effects of synthetic dyes, the use of discarded onion skins as a visual indicator of food freshness is a fine example of recycling and promoting the circular economy. In addition, the solvent-free synthesis of the filler and the use of starch as a matrix make an important contribution to the overall goal of achieving an environmentally friendly film. The extract also has other advantages such as a powerful antioxidant and a discreet antimicrobial effect which make the film an active material. Due to the presence of the filler, the active function of OE can be enhanced by the possibility of loading HNT and LDH with other antimicrobials with the intention of increasing food shelf life and avoiding waste. Finally, the cyanidin stabilisation promoted by filler-OE interactions was found to be crucial in increasing the reliability of the sensor, and the colour change response in both acid and basic environments make it a highly versatile packaging.

Acknowledgements: Project Prin 2017 "MultIFunctional poLymer cOmposites based on groWn matERials (MIFLOWER)" (grant number: 2017B7MMJ5_001) from the Italian Ministry of University and Research is kindly acknowledged

References

[1] D. Schaefer, W.M. Cheung, Smart Packaging: Opportunities and Challenges, Procedia CIRP. 72 (2018) 1022–1027. https://doi.org/10.1016/J.PROCIR.2018.03.240.

[2] K.B. Biji, C.N. Ravishankar, C.O. Mohan, T.K. Srinivasa Gopal, Smart packaging systems for food applications: a review, J. Food Sci. Technol. 52 (2015) 6125–6135. https://doi.org/10.1007/S13197-015-1766-7/TABLES/2.

[3] V. Shukla, G. Kandeepan, M.R. Vishnuraj, A. Soni, Anthocyanins based indicator sensor for intelligent packaging application, Agric. Res. 5 (2016) 205–209. https://doi.org/10.1007/S40003-016-0211-0.

[4] S. Huang, Y. Xiong, Y. Zou, Q. Dong, F. Ding, X. Liu, H. Li, A novel colorimetric indicator based on agar incorporated with Arnebia euchroma root extracts for monitoring fish freshness, Food Hydrocoll. 90 (2019) 198–205. https://doi.org/10.1016/J.FOODHYD.2018.12.009.

[5] Z. Aghaei, B. Ghorani, B. Emadzadeh, R. Kadkhodaee, N. Tucker, Protein-based halochromic electrospun nanosensor for monitoring trout fish freshness, Food Control. 111 (2020) 107065. https://doi.org/10.1016/J.FOODCONT.2019.107065.

[6] S. Kang, H. Wang, M. Guo, L. Zhang, M. Chen, S. Jiang, X. Li, S. Jiang, Ethylene-vinyl Alcohol Copolymer-Montmorillonite Multilayer Barrier Film Coated with Mulberry Anthocyanin for Freshness Monitoring, J. Agric. Food Chem. 66 (2018) 13268–13276. https://doi.org/10.1021/ACS.JAFC.8B05189/SUPPL_FILE/JF8B05189_SI_001.PDF.

[7] M. Weston, R.P. Kuchel, M. Ciftci, C. Boyer, R. Chandrawati, A polydiacetylene-based colorimetric sensor as an active use-by date indicator for milk, J. Colloid Interface Sci. 572 (2020) 31–38. https://doi.org/10.1016/J.JCIS.2020.03.040.

[8] H. zhi Chen, M. Zhang, B. Bhandari, Z. Guo, Applicability of a colorimetric indicator label for monitoring freshness of fresh-cut green bell pepper, Postharvest Biol. Technol. 140 (2018) 85–92. https://doi.org/10.1016/J.POSTHARVBIO.2018.02.011.

[9] M. Vanderroost, P. Ragaert, F. Devlieghere, B. De Meulenaer, Intelligent food packaging: The next generation, Trends Food Sci. Technol. 39 (2014) 47–62. https://doi.org/10.1016/J.TIFS.2014.06.009.

[10] E. Boccalon, G. Viscusi, A. Sorrentino, F. Marmottini, M. Nocchetti, G. Gorrasi, Solvent-free synthesis of halloysite-layered double hydroxide composites containing salicylate as novel, active fillers, Colloids Surfaces A Physicochem. Eng. Asp. 627 (2021) 127135. https://doi.org/10.1016/J.COLSURFA.2021.127135.

[11] C. Chen, M. Yang, Q. Wang, J.C. Buffet, D. O'Hare, Synthesis and characterisation of aqueous miscible organic-layered double hydroxides, J. Mater. Chem. A. 2 (2014) 15102–15110. https://doi.org/10.1039/C4TA02277G.

[12] A. Singh, Y. Gu, S.D. Castellarin, D.D. Kitts, A. Pratap-Singh, Development and Characterization of the Edible Packaging Films Incorporated with Blueberry Pomace, Foods 2020, Vol. 9, Page 1599. 9 (2020) 1599. https://doi.org/10.3390/FOODS9111599.

[13] C. Pagano, M. Marinozzi, C. Baiocchi, T. Beccari, P. Calarco, M.R. Ceccarini, M. Chielli, C. Orabona, E. Orecchini, R. Ortenzi, M. Ricci, S. Scuota, M.C. Tiralti, L. Perioli, Bioadhesive Polymeric Films Based on Red Onion Skins Extract for Wound Treatment: An Innovative and Eco-Friendly Formulation, Mol. 2020, Vol. 25, Page 318. 25 (2020) 318. https://doi.org/10.3390/MOLECULES25020318.

[14] L. Yang, Y. Xia, S.A. Junejo, Y. Zhou, Composition, structure and physicochemical properties of three coloured potato starches, Int. J. Food Sci. Technol. 53 (2018) 2325–2334. https://doi.org/10.1111/IJFS.13824.

[15] V. Vuiblet, T.T. Nguyen, A. Wynckel, M. Fere, L. Van-Gulick, V. Untereiner, P. Birembaut, P. Rieu, O. Piot, Contribution of Raman spectroscopy in nephrology: A candidate technique to detect hydroxyethyl starch of third generation in osmotic renal lesions, Analyst. 140 (2015) 7382–7390. https://doi.org/10.1039/c5an00821b.

[16] M.R. Almeida, R.S. Alves, L.B.L.R. Nascimbem, R. Stephani, R.J. Poppi, L.F.C. De Oliveira, Determination of amylose content in starch using Raman spectroscopy and multivariate calibration analysis, Anal. Bioanal. Chem. 397 (2010) 2693–2701. https://doi.org/10.1007/S00216-010-3566-2.

[17] X. Hu, J. Shi, F. Zhang, X. Zou, M. Holmes, W. Zhang, X. Huang, X. Cui, J. Xue, Determination of Retrogradation Degree in Starch by Mid-infrared and Raman Spectroscopy during Storage, Food Anal. Methods. 10 (2017) 3694–3705. https://doi.org/10.1007/S12161-017-0932-0.

[18] R. Kizil, J. Irudayaraj, Applications of Raman Spectroscopy for Food Quality Measurement, Nondestruct. Test. Food Qual. (2008) 143–163. https://doi.org/10.1002/9780470388310.CH6.

[19] H. Schulz, M. Baranska, Identification and quantification of valuable plant substances by IR and Raman spectroscopy, Vib. Spectrosc. 43 (2007) 13–25. https://doi.org/10.1016/J.VIBSPEC.2006.06.001.

[20] L.S. Guinesi, A.L. da Róz, E. Corradini, L.H.C. Mattoso, E. de M. Teixeira, A.A. d. S. Curvelo, Kinetics of thermal degradation applied to starches from different botanical origins by non-isothermal procedures, Thermochim. Acta. 447 (2006) 190–196. https://doi.org/10.1016/J.TCA.2006.06.002.

[21] J.K. Pandey, R.P. Singh, Green Nanocomposites from Renewable Resources: Effect of Plasticizer on the Structure and Material Properties of Clay-filled Starch, Starch - Stärke. 57 (2005) 8–15. https://doi.org/10.1002/STAR.200400313.

[22] C.L. Luchese, V.F. Abdalla, J.C. Spada, I.C. Tessaro, Evaluation of blueberry residue

incorporated cassava starch film as pH indicator in different simulants and foodstuffs, Food Hydrocoll. 82 (2018) 209–218. https://doi.org/10.1016/J.FOODHYD.2018.04.010.

[23] H. Cakmak, E. Sogut, Functional Biobased Composite Polymers for Food Packaging Applications, React. Funct. Polym. Vol. One. (2020) 95–136. https://doi.org/10.1007/978-3-030-43403-8_6.

[24] J. Bedrníček, J. Kadlec, I. Laknerová, J. Mráz, E. Samková, E. Petrášková, L. Hasoňová, F. Vácha, V. Kron, P. Smetana, Onion Peel Powder as an Antioxidant-Rich Material for Sausages Prepared from Mechanically Separated Fish Meat, Antioxidants 2020, Vol. 9, Page 974. 9 (2020) 974. https://doi.org/10.3390/ANTIOX9100974.

[25] D. Domene-López, J.C. García-Quesada, I. Martin-Gullon, M.G. Montalbán, Influence of Starch Composition and Molecular Weight on Physicochemical Properties of Biodegradable Films, Polymers (Basel). 11 (2019). https://doi.org/10.3390/POLYM11071084.

[26] L. Prietto, T.C. Mirapalhete, V.Z. Pinto, J.F. Hoffmann, N.L. Vanier, L.T. Lim, A.R. Guerra Dias, E. da Rosa Zavareze, pH-sensitive films containing anthocyanins extracted from black bean seed coat and red cabbage, LWT. 80 (2017) 492–500. https://doi.org/10.1016/J.LWT.2017.03.006.

[27] M. Sohany, I.S.M.A. Tawakkal, S.H. Ariffin, N.N.A.K. Shah, Y.A. Yusof, Characterization of Anthocyanin Associated Purple Sweet Potato Starch and Peel-Based pH Indicator Films, Foods 2021, Vol. 10, Page 2005. 10 (2021) 2005. https://doi.org/10.3390/FOODS10092005.

[28] X. Zhai, J. Shi, X. Zou, S. Wang, C. Jiang, J. Zhang, X. Huang, W. Zhang, M. Holmes, Novel colorimetric films based on starch/polyvinyl alcohol incorporated with roselle anthocyanins for fish freshness monitoring, Food Hydrocoll. 69 (2017) 308–317. https://doi.org/10.1016/J.FOODHYD.2017.02.014.

[29] J. Santas, M.P. Almajano, R. Carbó, Antimicrobial and antioxidant activity of crude onion (Allium cepa, L.) extracts, Int. J. Food Sci. Technol. 45 (2010) 403–409. https://doi.org/10.1111/J.1365-2621.2009.02169.X.

[30] N.A. Sagar, S. Pareek, S. Sharma, E.M. Yahia, M.G. Lobo, Fruit and Vegetable Waste: Bioactive Compounds, Their Extraction, and Possible Utilization, Compr. Rev. Food Sci. Food Saf. 17 (2018) 512–531. https://doi.org/10.1111/1541-4337.12330.

[31] J. Lachman, D. Proněk, A. Hejtmánková, J. Dudjak, V. Pivec, K. Faitová, Total polyphenol and main flavonoid antioxidants in different onion (Allium cepa L.) varieties, Hortic. Sci. 30 (2018) 142–147. https://doi.org/10.17221/3876-HORTSCI.

[32] W. Wiczkowski, J. Romaszko, A. Bucinski, D. Szawara-Nowak, J. Honke, H. Zielinski, M.K. Piskula, Quercetin from shallots (Allium cepa L. var. aggregatum) is more bioavailable than its glucosides, J. Nutr. 138 (2008) 885–888. https://doi.org/10.1093/JN/138.5.885.

[33] V. Benítez, E. Mollá, M.A. Martín-Cabrejas, Y. Aguilera, F.J. López-Andréu, K. Cools, L.A. Terry, R.M. Esteban, Characterization of industrial onion wastes (Allium cepa L.): dietary fibre and bioactive compounds, Plant Foods Hum. Nutr. 66 (2011) 48–57. https://doi.org/10.1007/S11130-011-0212-X.

[34] Y. Duan, D.-H. Jin, H.-S. Kim, J.-H. Seong, Y.-G. Lee, D.-S. Kim, H.-S. Chung, S.-H. Jang, Analysis of Total Phenol, Flavonoid content and Antioxidant Activity of Various Extraction Solvents Extracts from Onion (Allium cepa L.) Peels, J. Korean Oil Chem. Soc. 32 (2015) 418–426. https://doi.org/10.12925/JKOCS.2015.32.3.418.

[35] P.K. Sofia, R. Prasad, V.K. Vijay, A.K. Srivastava, Evaluation of antibacterial activity of

Indian spices against common foodborne pathogens, Int. J. Food Sci. Technol. 42 (2007) 910–915. https://doi.org/10.1111/J.1365-2621.2006.01308.X.

[36] M. Somrani, M.C. Inglés, H. Debbabi, F. Abidi, A. Palop, Garlic, Onion, and Cinnamon Essential Oil Anti-Biofilms' Effect against Listeria monocytogenes, Foods 2020, Vol. 9, Page 567. 9 (2020) 567. https://doi.org/10.3390/FOODS9050567.

[37] F. Fancello, G.L. Petretto, S. Marceddu, T. Venditti, G. Pintore, G. Zara, I. Mannazzu, M. Budroni, S. Zara, Antimicrobial activity of gaseous Citrus limon var pompia leaf essential oil against Listeria monocytogenes on ricotta salata cheese, Food Microbiol. 87 (2020) 103386. https://doi.org/10.1016/J.FM.2019.103386.

[38] G.L. Petretto, F. Fancello, K. Bakhy, C. AL Faiz, Z. Sibawayh, M. Chessa, S. Zara, M.L. Sanna, M. Maldini, J.P. Rourke, G. Pintore, Chemical composition and antimicrobial activity of essential oils from Cuminum cyminum L. collected in different areas of Morocco, Food Biosci. 22 (2018) 50–58. https://doi.org/10.1016/J.FBIO.2018.01.004.

[39] N.A. Sagar, S. Pareek, Antimicrobial assessment of polyphenolic extracts from onion (Allium cepa L.) skin of fifteen cultivars by sonication-assisted extraction method, Heliyon. 6 (2020) e05478. https://doi.org/10.1016/J.HELIYON.2020.E05478.

[40] D.N. Byrne, T.S. Bellows, Whitefly Biology, Http://Dx.Doi.Org/10.1146/Annurev.En.36.010191.002243. 36 (2003) 431–457. https://doi.org/10.1146/ANNUREV.EN.36.010191.002243.

[41] D. Amic, D. Davidovic-Amic, D. Beslo, V. Rastija, B. Lucic, N. Trinajstic, SAR and QSAR of the antioxidant activity of flavonoids, Curr. Med. Chem. 14 (2007) 827–845. https://doi.org/10.2174/092986707780090954.

[42] A.D. Diwan, A.S. Ninawe, S.N. Harke, Gene editing (CRISPR-Cas) technology and fisheries sector, Can. J. Biotechnol. 1 (2017) 65–72. https://doi.org/10.24870/CJB.2017-000108.

[43] M. Furusawa, T. Tanaka, T. Ito, A. Nishikawa, N. Yamazaki, K.I. Nakaya, N. Matsuura, H. Tsuchiya, M. Nagayama, M. Iinuma, Antioxidant Activity of Hydroxyflavonoids, J. Heal. Sci. 51 (2005) 376–378. https://doi.org/10.1248/JHS.51.376.